Organic Photonics and Photovoltaics
Research Article • DOI: 10.2478oph-2013-0004 • OPP • 2013 • 56-66

VERSITA

Functional π-conjugated polymers based on maleimide for photovoltaic applications

Abstract

A series of new bis-(2-thienyl) maleimide monomers have been synthesized and characterized. The bis-(2-thienyl)maleimide unit has been copolymerized with different aromatic comonomers. Stille coupling polymerizations under various conditions have been utilized. The copolymers were then characterized by size-exclusion chromatography and their optical and electronic properties were investigated by UV-Vis absorption spectroscopy and cyclic voltammetry. All maleimide based copolymers shared similar LUMO energy levels, which are largely determined by the acceptor moiety, and are close to that of $PC_{61}BM$ to be effective for charge dissociation. These low band gap polymers have been tested for photovoltaic applications and have shown moderate photovoltaic performance. Interesting results were obtained by adding the polymer to the P3HT:$PC_{61}BM$ mixture, as a third component. The ternary blend BHJ solar cells showed power conversion efficiencies of 35% exceeding those of the corresponding binary blends.

Keywords

Maleimide • OPV • ternary blends • photovoltaic • organic

PACS: 78.66.Sq; 82.70.Uv; 78.35.+c; 81.07.Pr; 88.40.jr

Ramona Gironda[1,2], Luciano Miozzo[1,2], Denis Tondelier[1], Marc Chaigneau[1], Jamal Ghabboun[3,4], Maryam Faroun[3], Antonio Papagni[2], Marco Matteo Salamone[2], and Riccardo Ruffo[2], Abderrahim Yassar*[1]

1 *LPICM, UMR 7647 CNRS, Ecole polytechnique, route de Saclay, 91128 Palaiseau Cedex, France*

2 *Dipartimento di Scienza dei Materiali, Universitŕ di Milano Bicocca, via R. Cozzi, 53, 20125, Milano, Italy*

3 *The Nanotechnology Research laboratory, Materials Engineering Department, Al-Quds University, East Jerusalem, Palestine*

4 *Department of Physics, Bethlehem University, Bethlehem, Palestine*

Received 05/13/2013
Accepted 09/25/2013

1. Introduction

Bulk heterojunction (BHJ) solar cells based on blend of conjugated polymer/fullerene systems offer promise for the realization of low-cost, printable, portable and flexible renewable energy sources. BHJ solar cell performance has progressively improved since their introduction [1] with power conversion efficiencies (PCE) now close to 10% [2]. Further enhancements of PCE and durability, together with the low-cost fabrication, are still required for commercial applications. Over the past decade, research has focused on regioregular poly(3-hexylthiophene) (P3HT) as the standard electron-donating material in polymer BHJ solar cells, with important progress having been made in understanding the device science and the associated improvements in device efficiency. However, P3HT is not the ideal polymer as it has a relatively large band gap (1.85 eV) and its high-lying highest occupied molecular orbital (HOMO) (−5.1 eV) limits the open circuit voltage (V_{oc}) of P3HT/(6,6)-phenyl-C61-butyric acid methyl ester ($PC_{61}BM$) devices to 0.6 V, consequently limiting the efficiency to about 5%. To overcome these limitations, low band gap materials with broad absorption spectra to enhance sunlight harvest for higher short circuit current (J_{sc}), an appropriately lower HOMO energy level to maximize the V_{oc}, a higher hole mobility for higher J_{sc} and higher fill factor (FF), have been proven to be an efficient strategy to improve device performance. Typically, a low band gap polymer is designed via donor-acceptor (D-A) approach by incorporating both electron-rich and electron-deficient moieties in the same conjugated backbone [3–5]. Among a wide variety of acceptor units, aromatic diimide units have been shown to be an excellent building block for the synthesis of low-bandgap conjugated polymers because they combine a deep lying HOMO, a rigid planar core and high electron mobility [6–9].

Using diimide derivatives, several research groups have synthesized D–A low-bandgap copolymers and reported the photovoltaic properties of those copolymers.

*E-mail: abderrahim.yassar@polytechnique.edu

For instance, thieno[3,4-c]pyrrole-4,6-dione (TPD) has been reported to be one of the most efficient building block thanks to some property, such as rigidity, good solubility and favorable 3D arrangement in the solid state. TPD-based polymers demonstrated PCEs as high as 8.5% [10]. Dithieno[3,2-*f*:2′,3′-*h*]phthalimide, a fused-ring compound, was also investigated as viable building blocks for low band gap materials for photovoltaic applications. The copolymers exhibited a broad absorption band with an absorption edge close to 700 nm and a PCE of 2 % when blended with $PC_{61}BM$ [11]. Jeneke et al. demonstrated BHJ cells based on blends of the new low band gap donor–acceptor copolymer, poly(N-(dodecyl)-3,6-bis(4-dodecyloxythiophen-2-yl)phthalimide) (PhBT12), and fullerene derivative ($PC_{61}BM$ or $PC_{71}BM$) [12]. The PhBT12/fullerene blend films were found to exhibit crystalline nanoscale morphology, with space-charge-limited mobility of holes as high as 4.0 10^{-4} cm^2/Vs without thermal annealing, leading to moderately efficient devices. The performance of the solar cells varied significantly with PhBT12/fullerene composition, reaching a PCE of 2.0% with a current density of 6.43 mA/cm^2 and a fill factor of 0.55 for the 1:1 PhBT12/$PC_{71}BM$ blend devices.

The common structural features of the aromatic diimides are (a) extended aromatic ring flanked in both sides by carboxylic diimides and (b) their powerful electron accepting ability. Maleimide has the simplest structure within unsaturated imide family and can be regarded as a *cis* olefin bisubstituted with an electron-withdrawing group, carboxylic imide. In spite of its simple structure, it is quite surprising that only a few attempts have been made to explore the possibility of using maleimide as building block of functional materials for organic electronics. In these regards, two different group of researcher reported the synthesis and characterization of a series of diphenylmaleimide-based π-conjugated copolymers with high red fluorescence both in solution and thin films [13, 14]. Chen et al. [13] synthetized and characterized homopolymer containing electrontransporting 1,2-diphenylmaleimide chromophores and copolymers consisting of 1,2-diphenylmaleimide and hole-transporting 2,5-thiophene moieties. In the second case, Chen et al. [14] designed 3,4-diphenylmaleimide-based π-conjugated copolymers obtaining different properties by varying the structural combination of thiophene and/or fluorene with 3,4-diphenylmaleimide fluorophore. Polymer light-emitting diodes fabricated from 3,4-diphenylmaleimide copolymer exhibited long wavelength electroluminescence from orange to the saturated red region, with satisfactory brightness and efficiency. Recently, and during the preparation process of the current work, Lee et al. reported the photovoltaic properties of cross-linkable maleimide/thiophene copolymers [15]. More recently, a series of D-A copolymers based on 3,4-diphenyl-maleimide has been presented for applications in polymer solar cells [16]. The HOMO level of these polymers were in the range of 5.63 – 5.73 eV, indicating the possibility to achieve a high V_{oc}. BHJSCs were prepared by blending them with $PC_{61}BM$ and $PC_{71}BM$. The best results were obtained with the device containing $PC_{71}BM$, with a V_{oc} of 0.74 V, J_{sc} of 7.4 mA cm^{-2}, a FF of 0.22 and a PCE of 1.20% under AM 1.5 G simulated solar light. The best device obtained with $PC_{61}BM$ gave a V_{oc} of 0.80 V, J_{sc} of 4.9 mA cm^{-2}, a FF of 0.21 and a PCE of 0.82%. In general, device performances based on these copolymers were limited by poor charge transport and light induced charge separation, but also confirm the interest in maleimide as accepting unit.

Herein, we present the synthesis of new D-A molecules and polymers containing bithienyl-maleimide units as electron acceptors and electron-rich thiophene units with the results of their optical, electrochemical, morphological and photovoltaic properties. Soluble oligomeric compounds were also synthesized via analogous organometallic coupling reaction. The compounds display well-defined conjugation length and provide simple model system for elucidating pertinent structure-property correlations, especially with respect to its photovoltaic behaviour.

2. Results and discussion

2.1. Materials Synthesis

Various synthetic procedures for preparing symmetrical or unsymmetrical 3,4-substituted maleimides are known. Previously, diaryl-maleimides were commonly synthesized from acetonitrile derivatives, however the yields were not satisfactory with thiophene [17, 18]. Alternative methods to prepare diaryl-maleimides or the corresponding diaryl-maleic anydrides or their precursors were based on a modified Perkin condensation involving sodium salts of arylglyoxylic acid and arylacetic acid with acetic anhydride [19], by oxidation of 2,5-dibromopyrrole in presence on HNO_3 [20] or variations of these methods [21–23]. The most direct way to access to bis(thien-2-yl) maleimides is based on the direct bromination of maleic anhydride with Br_2, catalyzed by $AlCl_3$ [24]. Dibromo-maleic anhydride is easily converted into the imide and the resulting compounds can be used in cross-coupling reactions to get access to bisaryl-maleimide [25–30]. To improve the yield of the reaction, we chose to apply an alternative method based on Stille coupling reaction [31]. 2,3-oligothiophene-N-substitued maleimide compounds (3, 5, and 6) were prepared by Stille coupling reaction start-

ing from 2,3-dibromo-N-octylmaleimide, using Pd^0 (generated from $Pd(PPh_3)_2Cl_2$) as catalyst (Scheme 1).

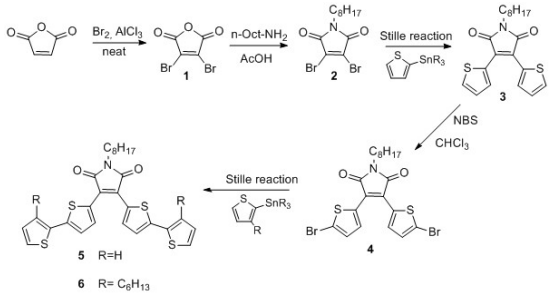

Sch. 1. Synthesis of 2,3-oligothiophene-N-substitued maleimide compounds.

The first step involves the bromination of neat maleic anhydride with Br_2 in the presence of catalytic amount of aluminum trichloride to provide 1 in good yield. The reaction of dibromo maleic anhydride with octyl amine, in acetic acid afforded to 3,4-dibromo-1-octyl-1H-pyrrole-2,5-dione (2) [24]. Coupling reaction of 2 with 2-(tributylstannyl)thiophene, using $PdCl_2(PPh_3)_2$ as a catalyst, lead to 2,3-dithiophene-N-octylmaleimide (3) in a good yield. The dibromination of compound 3 with an excess of NBS, in chloroform at r.t., provided the 2,3-bis(2-bromothiophene)-N-octylmaleimide (4) in 90% yield. To further extend oligothiophene chain we carried out the coupling reaction of compound 4 with 2-tributylstannylthiophene and 2-tributylstannyl-3-hexylthiophene, affording compounds 5 and 6, respectively.
All thienyl-maleimide derivatives were obtained in high purity after chromatography on silica gel. They were fully characterized by ^1H NMR and high-resolution mass spectroscopy confirmed the molecular weight for the compound 5. (See Exp. Section and Supplementary contents).

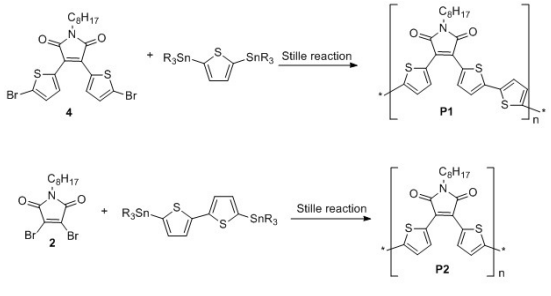

Sch. 2. Synthesis of copolymers based on maleimide.

In order to study the transformation of the maleimide derivatives into the new polymers P1 and P2, two coupling reactions were performed using bis-stannylthiophene and bis-stannyl-bis-thiophene. Scheme 2 shows the synthetic pathway to obtain polymers P1 and P2 by Stille reaction. The monomers 4 and 2 were reacted with bis(stannyl) derivatives using DMF and Pd^{II} as solvent and catalyst, respectively. The reaction mixture was heated overnight at 90°C in DMF.

The products were purified by re-precipitation from toluene into methanol and purified by Soxhlet extraction with MeOH and diethyl ether to remove residual catalyst and low molecular weight materials, respectively. All polymers show good solubility in halogenated solvents, such as chloroform and DCB. GPC in THF at RT was used to determine the molecular weights: the number-average molecular weights (Mn) and the polydispersity index (PI) of the P1 are 14,4 Kg/mol and 1,26, respectively while for the P2 are 11,6 Kg/mol and 1.45.

The GPC data confirm that the molecular weights of the polymers are very close to maleimide-based polymers already presented in literature prepared by Stille cross coupling [15].

2.2. Optical and Electrochemical Properties

The optical properties of P1, P2 and model compounds were investigated in solutions and thin films. The λ_{max} values for model compounds 3, 422 nm, is very close to those reported for (E)-1,2-bis(2-thienyl)vinylene and (E)-1,2-bis-[2,2'-bithienyl] vinylene, 422 and 435 nm respectively. This similarity suggests that introduction of the carboxylic imide onto the vinylene bridge has little influence on the electronic structure of the π-conjugated system [32]. Figure 1 shows the UV-visible absorption spectra of P2 in chloroform and thin film. In chloroform solution, it can be seen that P2 shows broad absorption between 300 and 700 nm with a maximum of 560 nm, which is the characteristic of the polythiophene derivatives. The absorption spectrum of the P2 film displays an absorption peak at 650 nm, which is red shifted by 90 nm in comparison with the absorption of polymer solution, indicating a strong intermolecular interaction in the polymer film. The optical bandgap of P2, calculated from the absorption edge in the UV–VIS spectrum of the thin film, is 1.55 eV.

The incorporation of maleimide electron deficient block in the polymers results in intra molecular charge transfer (ICT) between donor (thiophene) and acceptor, causing electronic delocalization along the polymer backbones. P2 shows a 180 nm bathochromic shift with respect to the previously reported conjugated copolymer based on 3,4-diphenyl-maleimide (λ_{max} = 450 nm) [13, 16]. The larger peak shift and the broadened absorption of P2 are ascribed to the much stronger ICT between the thiophene electron-donating unit and maleimide dicarboxylic imide

acceptor unit in P2 than that between phenyl donor and maleimide acceptor, previously reported.

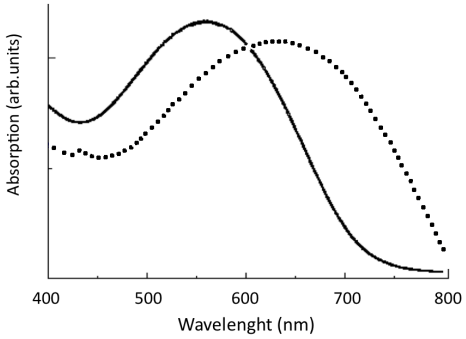

Fig. 1. UV-visible absorption spectrum of P2 (dotted line: thin film; solid line: chloroform solution).

The electrochemical properties of the model compound 5 were examined by cyclic voltammetry (CV) to estimate the HOMO and LUMO energy levels. The corresponding potential profiles are reported in Figure 2a (4 cycles). When the potential is scanned firstly just in the cathodic region, a reversible and stable redox process is present at potential ($E_{1/2}$) of −1.25 V vs. Fc. This process is attributed to the compound reduction in solution with the formation of the corresponding radical anion. On the contrary, when higher potential are explored in the anodic scan, an irreversible current peak is detected at 0.70 V vs. Fc, which is due to the oxidation of the neutral compound to the radical cation. After the first cycle, the peak current grows cycle by cycle and a new redox process is observed at lower potential (between 0.40 and 0.65 V) which can be attributed to the p-doping/de-doping of a semiconducting polymer growing at the electrode surface. So it is evident that the fresh formed radical cations react chemically to give polymer chains attached to the electrode. To further confirm this hypothesis, we have also characterized the obtained film by cyclic voltammetry in monomer free solution. The results are shown in Figure 2b where the characteristic p- and n-doping behaviors of a conducting polymer can be observed. As expected, the p-doping/dedoping process lies at potential lower than the corresponding monomer oxidation, while the polymer n-doping takes place at almost the same potential of the monomer reduction. In any case, both the polymer redox processes are reversible and no changes in the current profiles were observed after the first cycle.

The HOMO and LUMO energy levels of the compound 5 can be estimated from the current onset of the irreversible oxidation process at the first cycle and the $E_{1/2}$ value of the reversible reduction process, respectively. Potential

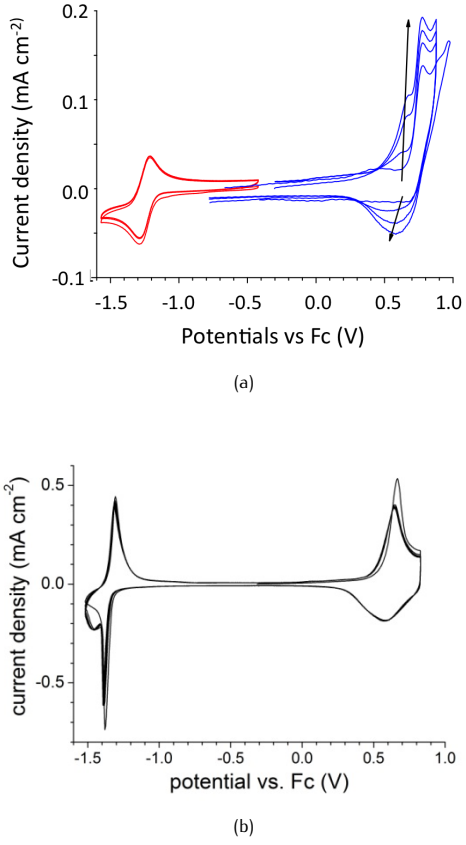

Fig. 2. a) Top: cyclic voltammetry curves of model compound 5 in solution. b) Bottom: cyclic voltammetry curves of poly-5 in monomer free solution.

values vs. Fc are converted to vacuum scale energies under the assumption that the Fc/Fc+ redox couple is 5.23 eV relative to a vacuum (using a potential value of 4.6 ± 0.2 eV for NHE vs. vacuum). The same procedure can also be used to calculate the polymer energy levels.

The HOMO and LUMO levels determined for the compound 5 are −5.9 and −4.0 eV, respectively; therefore its energy levels are between those of P3HT and $PC_{61}BM$, as reported in Figure 3. These values suggest the utilization of the small molecule as additive, in order to obtain an energy levels cascade and improved optical absorption.

The corresponding values for the polymer obtained electrochemically are −5.8 and −3.9 eV, respectively. The reduction potentials of the model compound is quite close to that of $PC_{61}BM$, with an offset of 0.2 eV (the $PC_{61}BM$ LUMO level was determined as −4.2 eV in our lab. under the same experimental conditions).

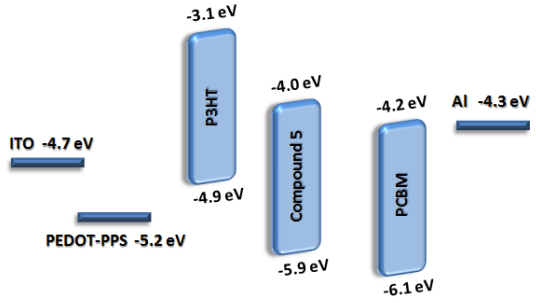

Fig. 3. Energy level diagrams for P3HT, 5 and $PC_{61}BM$.

2.3. Photovoltaic Properties and morphological analysis

Organic solar cells based on blends of $PC_{61}BM$, as electron acceptor, and P1 and P2, as electron donors, were fabricated with the common structure of ITO / PEDOT:PSS / polymer: $PC_{61}BM$ / LiF / Al. Solar cell devices were characterized under AM1.5G illumination at 100 mW/cm^2 with a solar simulator. The photovoltaic performances of the devices with different polymer / $PC_{61}BM$ weight ratio were investigated.

Small molecule containing the maleimide core was employed in 5:$PC_{61}BM$ blend system but any photovoltaic behavior was observed, because of the lack of the offset of the LUMO levels between 5 and $PC_{61}BM$. The offset is 0.2 eV, which is slightly lower than the minimum value required for efficient charge separation at the interface of the donor and acceptor; while in the case of the polymers the value of the LUMO levels are high enough to allow the excitons dissociation. Indeed when polymers were blended with $PC_{61}BM$ and used as active layer in device, a very small photovoltaic effect is observed. The device exhibited a J_{sc} of 0.11 mA/cm^2, a V_{oc} of 0.62 V, a FF of 0.22, and thus a PCE of 0.02%. The lower PCE and poor photovoltaic performance are in accordance with the literature for maleimide-based polymers.

The low J_{sc} could be attributed to the low LUMO offset between donor and acceptor, but also to the large-scale phase separation, which causes also, inefficient exciton dissociation.

The nanoscale morphology of the film was investigated by IC-AFM. Figure 4 shows the topography and the phase IC-AFM images for the P2:$PC_{61}BM$ annealed film with blend ratios of 1:1. The IC-AFM phase contrast image exhibits blend segregation and spherical aggregates are observed. The bright contrast corresponding to P2 clusters emerge from sample surface; the aggregate dimension, as reported in Figure 4, cannot be more than 400 nm because the dimension of the pores filter used blocks the bigger clusters. The presence of these aggregates can be ascribed to the limited solubility of P2.

The size of these domains is larger than the exciton diffusion length and their presence can be the origin of the poor results obtained with this materials. Attempts have been made to optimize these devices, but performances were still poor.

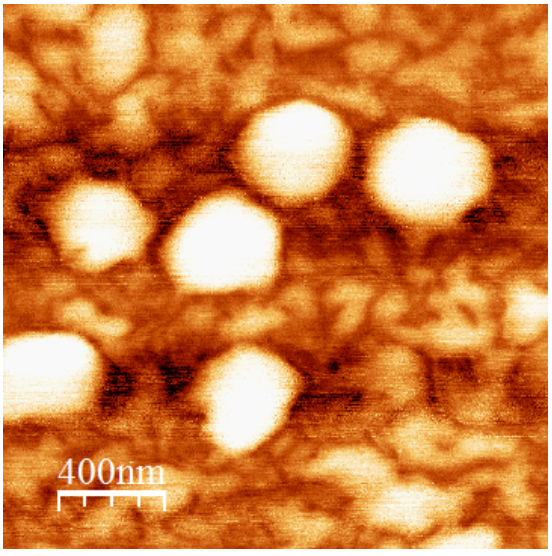

Fig. 4. IC-AFM (a) topography and (b) phase images of ITO/ PEDOT:PSS/P2: $PC_{61}BM$.

More interesting results were obtained by sensitizing the P3HT:$PC_{61}BM$ bulk heterojunction with compound 5 or polymers P1 and P2, as a third component. Several studies report improvement in the PCE of BHJ device based on P3HT:PCBM by incorporating additives via ternary mixing [33–35, 38].

For example, in terms of optimizing the performance of P3HT/PCBM in the BHJ solar cells, Chu and co-workers have applied a small molecule to form a ternary cascade structure, [36] resulting in about a 15% increase in PCE compared to a pristine P3HT:PCBM device. The offset of the energy levels of the donor and the acceptor normally gives to energy losses upon exciton dissociation and the addition of the third component can decrease the charge transfer barriers within the active layer and the recombination of the excitons could be significantly reduced.

For the third semiconductor, as the additive, three criteria must be respected: (i) its energy levels must have the proper offset with respect to P3HT and PCBM, the blend counterparts, (ii) it should be able to operate as either an electron acceptor and transporter as well electron donor and transporter, (iii) it should have an high absorption in the range complementary to the other components of the BHJ blend [36, 37].

The ternary blend films were prepared in proportions similar to the feed ratio of the P3HT:$PC_{61}BM$, binary blend system.

Fig. 5 shows the J–V characteristics of the P3HT:P2:$PC_{61}BM$ ternary blend solar cells and the corresponding P3HT:$PC_{61}BM$ binary blend control device. The ternary blend solar cells exhibited a substantially improved performance compared to the binary blend control device. Hence, devices fabricated using P3HT:P2:$PC_{61}BM$ (0.8:0.2:1) showed considerably enhanced performance (Figure 5, red line) with a PCE of 3.14% compared to the P3HT:$PC_{61}BM$ control device. The addition of P2 increased the PCE from 1.73 to 3.14%, an 80% improvement. The performance improvement from the P3HT: $PC_{61}BM$ to the P3HT:P2: $PC_{61}BM$ systems is mainly attributed to the increase in both J_{sc} (from 7.2 to 9.9 mA cm^{-2}) and FF (from 0.41 to 0.51). This improvement, upon addition of P2, can be explained in terms of increased optical absorption and improved thin film morphology.

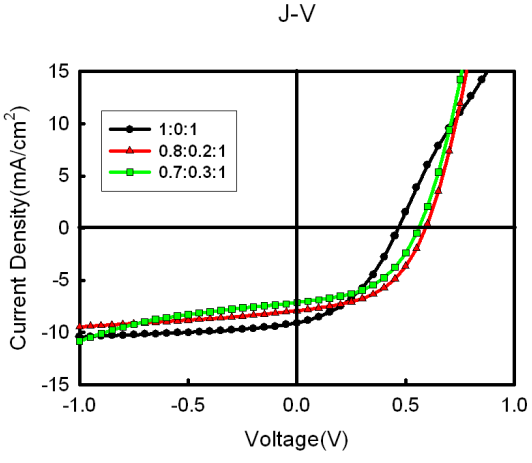

Fig. 5. I-V characteristic of ITO/PEDOT:PSS/P3HT:P2: $PC_{61}BM$ /LiF/Al with increasing amount of P2.

In S.I. are reported the absorbance spectra of ternary blend P3HT:P2:$PC_{61}BM$ films with P2 content from 0 wt% to 17 wt%. By increasing P2 ratio, the absorbance in the wavelength range of 750-600 nm is increased, due to the contribution of P2. The P3HT contribution decreases with the addition of P2 but stays then constant with increasing P2 content. The decreasing of the P3HT absorption is due to a lower amount of P3HT in the film. Moreover, the shoulders at 594 nm, which arises from crystalline regions do not change with the P2 content. Consequently, the P2 chains do not incorporate in the crystalline domains but in the amorphous regions of P3HT. To probe the underlying cause of the origin of the increase in J_{sc} by the addition of P2, we performed the EQE spectra of P3HT:P2:$PC_{61}BM$ devices (See Supporting contents). In the normalized EQE spectra of the P3HT:P2:$PC_{61}BM$ devices the photocurrent peak in the wavelength range of the P2 absorption, increases as the P2 content increased, which is clear evidence that P2 contributes to the photocurrent.

In a second set of experiments, the third component in the ternary blend was the compound 5 and the content was varied over range of 0 to 16 wt%. Photovoltaic performances of devices produced with these multicomponent blend films, are presented in Table 1. Short-circuit current densities, J_{sc}, in the devices with the ternary blend films, were found increased highly when compared with those comprising the corresponding binary P3HT:$PC_{61}BM$.

Figure 6 displays J–V curves for devices incorporating different blend ratio of the three components compared to P3HT:$PC_{61}BM$ (1:1 w/w) as a reference, under simulated AM 1.5 G irradiation (100 mW/cm^2). The active layers were spin-coated from o-DCB solutions of PH3T, 5 and $PC_{61}BM$ and the detailed conditions of the device fabrication and characterization are described in the experimental section (Device Fabrication and Characterization). Two blends with different composition, P3HT:5:$PC_{61}BM$ 23:7:30 and 20:10:30 (% weight), were investigated, with a final thickness device of 120 nm. The blend P3HT:$PC_{61}BM$ was used as standard reference and shows a J_{sc} of 8.03 mA/cm^2, a V_{oc} of 0.60 V, a FF of 0.44 leading to PCE of 2.60%. The best performance is observed in the P3HT:5:$PC_{61}BM$ (23:7:30, w/w) blend, which shows an improved V_{oc} of 0.62 V and J_{sc} of 10.11 mA/cm^2, whereas the FF of 0.48 is similar to those of that obtained for the device lacking additive. The corresponding PCE is 35% higher relative to that of the pristine P3HT:$PC_{61}BM$. For concentrations of 5 greater than 10 wt% the device exhibited relatively lower current density. The lower J_{sc} values can be explained by the decreased order within the P3HT domains. The crystallinity of P3HT could be destroyed if the amount of additive is too much, that means unfavourable morphology of the active layer and charge transport lowered.

To gain more insight into the variations in the dependence of the photovoltaic behaviour on the blend compositions, IC-AFM images (topography and phase) of the blends were recorded and compared. Figure 7, (a) and (c) presents topographic IC-AFM images from which are derived the domain sizes and the roughness values announced. Rather than the topographic image, the phase IC-AFM (Fig. 7 (b) and (d)) is an effective tool to investigate phase separation and dispersion between P3HT and $PC_{61}BM$. The contrast in the IC-AFM phase images comes

Table 1. Photovoltaic performance of P3HT: $PC_{61}BM$ (1:1 w/w) device doped with different concentrations of 5.

Composition	J_{sc} ($mAcm^{-2}$)	V_{oc} (V)	FF	PCE (%)
P3HT: $PC_{61}BM$ 30:30 (w/w)	8.03	0.60	0.44	2.60
P3HT:5: $PC_{61}BM$ 23:7:30 (w/w)	10.11	0.62	0.48	3.51
P3HT:5: $PC_{61}BM$ 20:10:30 (w/w)	8.90	0.61	0.48	2.86

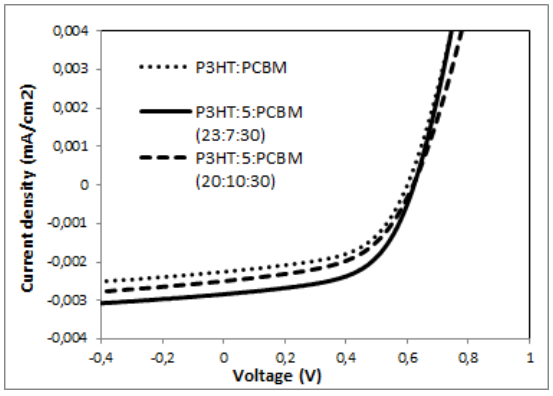

Fig. 6. J-V characteristic of ternary blend BHJ solar cell based on P3HT:5: $PC_{61}BM$ films with different ratios of 5.

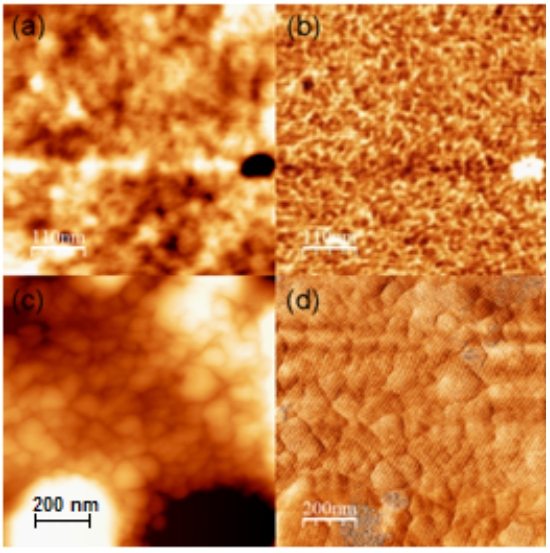

Fig. 7. (a) IC-AFM topographic image and (b) phase image of the top surface of the P3HT:$PC_{61}BM$:5/ 23:30:7 (wt 3%) film. (c) IC-AFM topographic image of the top surface of the P3HT:$PC_{61}BM$:5/ 20:30:10 (wt 3%) film. and (d) phase image of the top surface of the P3HT: $PC_{61}BM$:5/ 30:30:0 film.

from differences in the interaction between the materials and the tip.

When the P3HT:$PC_{61}BM$:5 ratios is 23:30:7, a clear phase contrast is observed, the IC-AFM phase image of the film (Fig. 7b) shows interpenetrating polymer networks for efficient charge separation and transport throughout the whole active layer. The sizes of the domains are in this case quite similar to the typical exciton diffusion length in a conjugated polymer (approximately 20-30 nm in nearly every points of the analysed surface). Hence, the electron donor and acceptor materials forms nanoscale interpenetrating networks. As a result, the better solar cell performances were obtained from this composition blend (23:30:7/P3HT:$PC_{61}BM$:5).

$PC_{61}BM$ molecules, at this concentration, are more uniformly dispersed than those prepared in the P3HT:$PC_{61}BM$/30:30 and P3HT:5:$PC_{61}BM$/20:10:30 composition.

For the 20:30:10/P3HT:$PC_{61}BM$:5 film, separated structure appeared effectively in the Figure 7 c), with domain size of about 100 nm to 200 nm. The spots with bright contrast in the topographic images represent the P3HT-rich phase. In contrast, flat surface without any distinct structure was observed in the AFM images of the 30:30:0/P3HT:$PC_{61}BM$:5 sample. No obvious phase separation exists at the surface of the blend film.

3. Experimental section

All chemicals were purchased from Aldrich chemical company and used without further purification. Anhydrous solvents were used for Stille reactions. Regioregular P3HT (55 kDa) was purchased from Aldrich or Merck and $PC_{61}BM$ (>99.5%) was obtained from Ossila. ^1H NMR spectra were recorded on a Bruker 500 (500 MHz) using TMS as an internal standard. Mass spectra were recorded on a GC-MS CLARIUS 560/600. HRMS analyses were performed on a JEOL GCMate II, using EI+ ionization.

Absorption spectra were recorded on a JASCO V-570 spectrophotometer at room temperature. Molecular weights (Mn, Mw) and polydispersity indexes (Mw/Mn) were measured by GPC on a Model Dionex UltiMate 3000, equipped with a pump, an absorbance detector (UV, $\lambda = 254$ nm), pre-columns filter and polystyrene gel columns based on a conventional calibration curve using polystyrene standards. THF was used as a carrier solvent at a flow rate of 1.0 mL/min at room temperature.

3.1. Electrochemical Characterization

Compound 5 was dissolved (5×10^{-4} M) in a 0.1 M solution of tetrabutylammonium perchlorate ($TBAClO_4$) (Fluka, electrochemical grade, >99.0%) in anhydrous acetonitrile (Aldrich, 99.8%). Cyclic Voltammetries (CV) were performed at a scan rate of 50 mV/s with a PARSTA2273 EG&G potentiostat in a three-electrode electrochemical cell. All the measurements were carried out in a glove box filled with argon ([O_2]<1 ppm). The working, counter, and pseudoreference electrodes were a well-polished Au pin, a Pt flag and a Ag/AgCl wire, respectively. The Ag/AgCl pseudoreference electrode was externally calibrated by adding ferrocene ($1x10^{-3}$ M) to the electrolyte. In the paper, all the potentials will be reported vs. the ferrocinium/ferrocene couple.

3.2. AFM Characterization

AFM measurements were performed using Nanotec Electronica microscope, operating in tapping mode or contact intermittent (IC-AFM). Scans were performed on areas close to the aluminium electrode. Both topographic and phase images are presented.

3.3. Device Fabrication and Characterization

All bulk-heterojunction photovoltaic cells were prepared using the same preparation procedures and device fabrication procedure referring as follows: glass-indium tin oxide ITO) substrates (obtained from Xinyan Technologies, ρ <20 Ω cm^{-2}) were first patterned by acid etching. Before processing, the patterned ITO glasses were cleaned by sonication, first in a microelectronic detergent, then in deionized water for 45 minutes, and finally rinsed by acetone and isopropyl alcohol. After dried by blowing nitrogen gas, substrates were irradiated in a UV-ozone chamber for 15 minutes. Poly(3,4-ethylenedioxy-thiophene):poly-(styrene-sulfonate) (PEDOT:PSS, Baytron 4083) was filtered through 0.4.µm filter before being deposited on ITO with a thickness around 40 nm by spin coating at 3500 rpm for 30s under nitrogen atmosphere, and dried at 108°C for 2 min inside a glove-box. Then, the active layer, made by P3HT: $PC_{61}BM$:5 with different ratios, was spin-coated from o-dichlorobenzene (DCB) solutions on the top of PEDOT:PSS layer at a speed rate of 1000 rpm for 45 s. The solar cell devices were completed by thermal evaporation of LiF (1.2 nm) and Al (100 nm) under 10^{-6} Torr pressure. The deposition rates of LiF and Al were 0.1 and 2.5 Å/s, respectively. The blend PEDOT:PSS was used to facilitate hole extraction and LiF was used for electron injection purposes. The active area of the device was 0.28 cm^2. The current-voltage (I-V) measurements of the polymer photovoltaic cells were carried out inside a dry box by a computer-controlled Keithley 2635 source measurement unit (SMU) with a solar simulator (SolarCell Test 575 from KHS) under the illumination of AM1.5G, 100 mW/cm^2. UV-Visible (JASCO V-570) spectra were measured for films of P3HT: $PC_{61}BM$ with and without additive.

3.4. Material Synthesis

3.4.1. Synthesis of 2,3-dibromo-maleic anhydride (1)

The reaction was carried out under solvent free conditions. In a round-bottomed flask, equipped with a magnetic stirring bar and a nitrogen inlet, were added maleic anhydride (10.0 g, 102 mmol) and aluminium trichloride (1.0 g, 7.5 mmol). The mix was melted and then cooled at r.t., then 2 eq.s of Br_2 (32.55 g, 203 mmol) were added in one portion and the reaction was stirred at 150°C overnight. After cooling to r.t., the solid was dissolved with ethyl acetate and the insoluble residue was filtered off. The solvent was removed under vacuum affording the desired product as white solid. Yield = 52%. M.p. and mass spectra were identical with those reported in literature.

3.4.2. Synthesis of 2,3-dibromo-N-octylmaleimide (2)

In a round-bottomed flask, equipped with a magnetic stirring bar and a nitrogen inlet, 1 equivalent of 2,3-dibromo-maleic anhydride (1, 5.0 g, 19.5 mmol) was dissolved in 25 mL of acetic acid. 1.5 eq.s of octylamine (3.78 g, 29.25 mmol) were added to the solution, which was refluxed for 12 hours under nitrogen atmosphere. After cooling at r.t., the mixture was added to saturated solution of $NaHCO_3$ (100 mL) and then extracted with ethyl acetate (100 mL x 3). After drying over anhydrous magnesium sulfate, the filtrate concentrated in vacuo. The residue was purified by rapid filtration on a silica bed, using CH_2Cl_2, to afford the desired product as red solid. Yield = 43%.

^1H NMR (500 MHz, $CDCl_3$, 300 K): δ (ppm) = 3.58 (t, 2H, N-CH_2, 1J = 7.0 Hz, 2J = 14 Hz), 1.58 (m, 2H, N-CH_2-$\underline{CH_2}$-), 1.30-1.24 (m, 10H, -CH_2-), 0.86 (t, 3H, CH_3, 1J = 7.5 Hz).

3.4.3. Synthesis of 2,3-dithiophen-N-octylmaleimide (3)

To a solution of 2,3-dibromo-N-octylmaleimide (2, 2.0 g, 5.4 mmol) and 2-(tributylstannyl)thiophene (4.06 g, 10.8 mmol) in 40 mL of DMF, $Pd(PPh_3)_2Cl_2$ (76 mg, 0.108 mmol, 2%) was added. The mixture was refluxed for 12 hours at 100°C under nitrogen atmosphere. After cooling at r.t., the mixture was added to water and extracted with toluene (50 mL x 3). After drying over anhydrous magnesium sulphate, the filtrate concentrated in vacuo. The crude product was purified by flash column chromatography (SiO_2, petroleum ether: ethyl ac-

etate 9:1) to afford the desired product as red oil. Yield = 91%

^{1}H NMR (500 MHz, $CDCl_3$, 300 K): δ (ppm) = 3.62 (t, 2H, N-CH_2, 1J = 7.0 Hz, 2J = 14.0 Hz), 1.65 (m, 2H, N-CH_2-$\underline{CH_2}$-), 1.35 (m, 10H, -CH_2-), 0.87 (t, 3H, CH_3, 1J = 6.5 Hz, 2J = 13.0 Hz), 7.58 (dd 2H, CH thiophene, 1J = 1 Hz, 2J = 5 Hz), 7.13 (t, 2H, CH thiophene, 1J = 4.5 Hz, 2J = 9 Hz), 7.82 (dd, 2H, CH thiophene, 1J = 1.5 Hz, 2J = 4 Hz).

MS: m/z: 373 [M+].

3.4.4. Synthesis of 2,3-bis(2-bromothiophen)-N-octylmaleimide (4)

In a round-bottomed flask, equipped with a magnetic stirring bar and a nitrogen inlet, 1 equivalent of 2,3-dithiophen-N-octylmaleimide (3, 1.5 g, 4.02 mmol) was dissolved in 30 mL of chloroform. 2.2 eq. of NBS (1.5 g, 8.84 mmol) were added portionwise to this solution, which was kept under stirring at r.t. overnight. The mixture was added to water (100 mL) and then extracted with chloroform (50 mL x 3). After drying over anhydrous magnesium sulphate, the filtrate concentrated in vacuo affording the desired product as orange solid. Yield = 90%.

^{1}H NMR (500 MHz, $CDCl_3$, 300 K): δ (ppm) = 3.59 (t, 2H, N-CH_2, 1J = 7 Hz, 2J = 14.0 Hz), 1.63 (m, 2H, N-CH_2-$\underline{CH_2}$-), 1.30 (m, 10H, -CH_2-), 0.87 (t, 3H, CH_3, 1J = 6.5 Hz, 2J = 13 Hz), 7.10 (d, 2H, CH thiophene, J = 4 Hz), 7.62 (d, 2H, CH thiophene, J = 4 Hz).

MS: m/z: 531.

3.4.5. Synthesis of 2,3-bis(5,2'-bithiophen-2-yl)-N-octylmaleimide (5)

To a solution of 2,3-bis(2-bromothiophen)-N-octylmaleimide (4) (0.5 g, 0.93 mmol) in 5 mL of dry DMF and 2-(tributylstannyl)thiophene (0.7 g, 1.9 mmol), $Pd(PPh_3)_2Cl_2$ (13 mg, 0.018 mmol, 2%) was added. The mixture was heated for 6 hours at 100°C under nitrogen. The reaction was monitored by TLC. After cooling to r.t., the mixture was added to water and extracted with ethyl acetate (50 mL x 3). After drying over anhydrous magnesium sulphate, the filtrate was concentrated in vacuo. The crude product was purified by flash column chromatography, (SiO_2, hexane: ethyl acetate 95 : 5) to afford the desired product as a purple solid. Yield = 60%.

^{1}H NMR (500 MHz, $CDCl_3$, 300 K): δ (ppm) = 3.60 (t, 2H, N-CH_2, 1J = 7.5 Hz, 2J = 14.0 Hz), 1.68-1.63 (m, 2H, N-CH_2-$\underline{CH_2}$-), 1.38-1.23 (m, 10H, -CH_2-), 0.88 (t, 3H, CH_3, 1J = 7.0 Hz, 2J = 14.0 Hz), 7.86 (d, 2H, CH thiophene, 1J = 4.0 Hz), 7.3 (m, 4H, CH thiophene), 7.20 (d, 2H, CH thiophene, 1J = 4.0 Hz), 7.05 (t, 2H, CH thiophene, 1J = 4.5 Hz, 2J = 8.5 Hz)

MS: m/z: 537.

3.4.6. Synthesis of 2,3-bis(3'-hexyl-5,2'-bithiophen-2-yl)-N-octylmaleimide (6)

To a solution of 2,3-bis(2-bromothiophen)-N-octylmaleimide (4) (1.00 g, 1.42 mmol) in 10 mL of dry DMF and 2-(tributylstannyl)-3-hexylthiophene (1.87 g, 5.64 mmol), $Pd(PPh_3)_2Cl_2$ (26 mg, 0.036 mmol, 2%) was added. The mixture was heated for 6 hours at 100°C under nitrogen. The reaction was monitored by TLC. After cooling to r.t., the mixture was added to water and extracted with toluene (50 mL x 3). After drying over anhydrous sodium sulphate, the filtrate was concentrated in vacuo. The crude product was purified by flash column chromatography, (SiO_2, hexane: ethyl acetate 9:1) to afford the desired product as purple oil. Yield = 81%.

^{1}H NMR (500 MHz, $CDCl_3$, 300 K): δ (ppm) = 3.63 (t, 2H, N-CH_2, 1J = 10 Hz, 2J = 15 Hz), 2.80 (t, 4H, Thiophene-CH_2, 1J = 5 Hz, 2J = 15 Hz), 1.67-1.61 (m, 6H), 1.38-1.23 (m, 22H), 0.89-0.86 (m, 9H, CH_3), 6.95 (d, 2H, CH thiophene, 1J = 5 Hz), 7.14 (d, 4H, CH thiophene, 1J = 5 Hz), 7.23 (d, 2H, CH thiophene, 1J = 5 Hz).

MS: m/z: 705.

3.4.7. Synthesis of poly (3-(2,2'-bithien-5-yl)-4-(thien-2-yl)-1-octyl-pyrrole-2,5-dione) (P1)

To a solution of 4 (200 mg, 0.38 mmol) and 2,5-bis(tributyl)stannyl-thiophene (270 mg, 0.41 mmol) dissolved in DMF (10 mL) $Pd(PPh_3)_2Cl_2$ (5 mg, 0.07 mmol, 2%) was added. The mixture was heated for 20 hours at 90°C under nitrogen atmosphere. The polymer was precipitated by pouring the DMF solution into methanol (200 mL). The crude product was filtered and then Soxhlet extracted with methanol and diethyl ether to remove the oligomers and catalyst residues until the extraction solution was colourless. 40 mg dark solid. Yield = 21%.

^{1}H NMR (500 MHz, $CDCl_3$, 300 K): δ (ppm) = 0.88 (br, 3H, CH_3), 1.27 (br, 6H, CH_2), 1.33 (br, 6H, CH_2), 3.62 (br, 2H, N-CH_2), 7.20 (br, 4H, CH thiophene), 7.88 (br, 2H, CH thiophene).

GPC (THF, 25 °C, RI Detector): Mn = 14397 g mol^{-1}, Mw = 18223 g mol^{-1}, Mp = 19432 g mol^{-1}, PDI = 1.26

λ_{max} (THF) = 590 nm.

3.4.8. Synthesis of poly(3,4-di(2,2'-bithien-5-yl)-1-octyl-pyrrole-2,5-dione) (P2)

To a solution of 2 (250 mg, 0,68 mmol) and 2,5-bis(trimethyl)stannyl-bithiophene (0,56 mg, 0,75 mmol) dissolved in DMF (10 mL) $Pd(PPh_3)_2Cl_2$ (9,6 mg, 0,14 mmol, 2%) was added. The mixture was heated for 20 hours at 90°C under nitrogen atmosphere. The polymer was precipitated by pouring the DMF solution into methanol (200 mL). The crude product was filtered and then Soxhlet extracted with methanol and diethyl ether to remove the oligomers and catalyst residues until the ex-

traction solution was colourless. 150 mg dark solid. Yield = 60%.

^{1}H NMR (500 MHz, $CDCl_3$, 300 K): δ (ppm) = 0.87 (br, 3H, CH_3), 1.25 (br, 6H, CH_2), 1.43 (br, 4H, CH_2), 1.57 (br, 4H, CH_2), 3.67 (br, 2H, N-CH_2), 6.98 (br, 2H, CH thiophene), 7.28 (br, 2H, CH thiophene).

GPC (THF, 25 °C, RI Detector): Mn = 11650 g mol^{-1}, Mw = 16940 g mol^{-1}, Mp = 19621 g mol^{-1}, PDI = 1.45

λmax ($CHCl_3$) = 561 nm

4. Conclusions

A series of polymers and model compounds based on maleimide, as electron poor moiety into the donor-acceptor structure, has been synthesized by simple and efficient route. The optical properties of the polymer show a stronger internal charge transfer between the thiophene (donor) and the (maleimide) acceptor blocks, which leads larger and broadened absorptions than previously reported for maleimide based polymers. Initial BHJ solar cell devices in combination with $PC_{61}BM$ give poor photovoltaic performance, which is mostly attributed to the limited solubility of the polymer, which produces in the active layer domains larger than the typical exciton diffusion length, as confirmed by AFM investigation.

However interesting results were obtained by sensitizing the P3HT:$PC_{61}BM$ bulk heterojunction with model compound 5 or polymer P2, as a third component. The addition of P2, as third component improved the PCE from 1.73 to 3.14%, an 80% increase. The same improvement has been obtained if a small molecule containing the maleimide core was added to the standard blend. The good match of the electronic levels between the three components together the suitable morphology of the film produce a PCE of 35% greater than the reference cell without additive.

Acknowledgements

A. Yassar and L. Miozzo wish to thank "Fondation de Coopération Scientifique "Campus Paris Saclay" (project 2011-087T -BlockSolarCell)" for financial support. L. Miozzo and R. Gironda wish to thank Andrea Sacchi for experimental contribution.

References

[1] G. Yu, J. Gao, J. C. Hummelen, F. Wudl and A. J. Heeger, *Science*, 1995, 270,1789.

[2] M. A. Green, K. Emery, Y. Hishikawa, W. Warta, E. D. Dunlop, *Progress in Photovoltaics: Research and Applications*, 2012, 20, 12.

[3] H. Zhou, L. Yang ,W. You, *Macromolecules*, 2012, 45, 607.

[4] P. M. Beaujuge, J. M. J. Fréchet, *Journal of the American Chemical Society*, 2011, 133, 20009.

[5] Y. Li, *Accounts of Chemical Research*, 2012, 45, 723.

[6] E. Zhou, J. Cong, Q. Wei, K. Tajima, C. Yang, K. Hashimoto, *Angewandte Chemie International Edition*, 2011, 50, 2799.

[7] X. Zhan, A. Facchetti, S. Barlow, T. J. Marks, M. A. Ratner, M. R. Wasielewski, S. R. Marder, *Advanced Materials*, 2011, 23, 268.

[8] X. Zha, X. Zhan, *Chemical Society Reviews*, 2011, 40, 3728.

[9] Y. Lin, Y. Li, X. Zhan, *Chemical Society Reviews*, 2012, 41, 4245.

[10] A. Pron, P. Berrouard , M. Leclerc, *Macromol. Chem. Phys.* 2013, 214, C. M. Amb. S. Chen, K R. Graham, J. Subbiah, C. E. Small, Franky So, J. R. Reynolds, *J. Am. Chem Soc.* 2011, *133*, 10062; X. Guo, N. Zhou, S. J. Lou, J. W. Hennek, R. Ponce Ortiz, M. R. Butler, P.-Luc T. Boudreault, J. Strzalka, P.-Olivier Morin, M. Leclerc, J. T. López Navarrete, M. A. Ratner, L. X. Chen, R. P. H. Chang, A Facchetti, T. J. Marks *J. Am. Chem Soc.* 2012, *134*, 18427; Ta-Ya Chu, J. Lu, S. Beaupré, Y. Zhang, J.-Rémi Pouliot, J. Zhou, A Najari, M. Leclerc, Y Tao, *Adv. Func. Mater.* 2012, 2345

[11] H. Wang, Q. Shi, Y. Lin, H. Fan, P. Cheng, X. Zhan, Y. Li, D. Zhu, *Macromolecules* 2011, 44, 4213.

[12] H. Xin, X. Guo, F. S. Kim, G. Ren, M. D. Watson and S. A. Jenekhe, *Journal of Materials Chemistry*, 2009, 19, 5303.

[13] T.-Z. Liu and Y. Chen, *Polymer*, 2005, 46, 10383.

[14] L.-H. Chan, Y.-D. Lee, C.-T. Chen, *Macromolecules*, 2006, 39, 3262.

[15] R.-H. Lee, J.-Y. Syu, J.-L. Huang, *Polymers for Advanced Technologies*, 2011, 22, 2110.

[16] L.-H. Chan, S.-Y. Juang, M.-C. Chen, Y.-J. Lin, *Polymer*, 2012, 53, 2334.

[17] H.-C. Yeh, W.-C. Wu, C.-T. Chen, *Chemical Communications*, 2003, 404.

[18] L.-H. Chan, Y.-D. Lee, C.-T. Chen, *Tetrahedron*, 2006, 62, 9541.

[19] H. Shih, R. J. Shih, D. A. Carson, *Journal of Heterocyclic Chemistry*, 2011, 48, 1243.

[20] D.-S. Choi, S. Huang, M. Huang, T. S. Barnard, R. D. Adams, J. M. Seminario, J. M. Tour, *The Journal of Organic Chemistry*, 1998, 63, 2646.

[21] E. M. Beccalli, M. L. Gelmi, A. Marchesini, *European Journal of Organic Chemistry*, 1999, 1421.

[22] A. Terpin, K. Polborn, W. Steglich, *Tetrahedron*, 1995, 51, 9941.

[23] E. K. Fields, S. J. Behrend, S. Meyerson, M. L.

Winzenburg, B. R. Ortega and H. K. Hall, *The Journal of Organic Chemistry*, 1990, 55, 5165.
[24] M. Dubernet, V. Caubert, J. Guillard, M.-C. Viaud-Massuard, *Tetrahedron*, 2005, 61, 4585.
[25] H. Wang, Q. Shi, Y. Lin, H. Fan, P. Cheng, X. Zhan, Y. Li, D. Zhu, *Macromolecules*, 2011, 44, 4213.
[26] P. S. Deore, N. P. Argade, *The Journal of Organic Chemistry*, 2011, 77, 739.
[27] K. Onimura, M. Matsushima, M. Nakamura, T. Tominaga, K. Yamabuki, T. Oishi, *Journal of Polymer Science Part A: Polymer Chemistry*, 2011, 49, 3550.
[28] K. Onimura, M. Matsushima, K. Yamabuki, T. Oishi, *Polym. J.*, 2010, 42, 290.
[29] S. Shorunov, M. Krayushkin, F. Stoyanovich, M. Irie, *Russian Journal of Organic Chemistry*, 2006, 42, 1490.
[30] C. Marminon, A. Pierré, B. Pfeiffer, V. Pérez, S. Léonce, P. Renard, M. Prudhomme, *Bioorganic & Medicinal Chemistry*, 2003, 11, 679.
[31] D. Waghray, W. Nulens, W. Dehaen, *Organic Letters*, 2011, 13, 5516.
[32] P. Frčre, J.-M. Raimundo, P. Blanchard, J. Delaunay, P. Richomme, J.-L. Sauvajol, J. Orduna, J. Garin, J. Roncali, *The Journal of Organic Chemistry*, 2003, 68, 7254.
[33] S. Sista, Y. Yao, Y. Yang, M. L. Tang, Z. Bao, *Applied Physics Letters*, 2007, 91, 223508.
[34] E. Lim, S. Lee, K. K. Lee, *Chemical Communications*, 2011, 47, 914.
[35] J. Lee, M. H. Yun, J. Kim, J. Y. Kim, C. Yang, *Macromolecular Rapid Communications*, 2012, 33, 140.
[36] J.-H. Huang, M. Velusamy, K.-C. Ho, J.-T. Lin, C.-W. Chu, *Journal of Materials Chemistry*, 2010, 20, 2820.
[37] M.C. Chen, D.J. Liaw, Y.C. Huang, H.Y. Wu, Y. Tai, Solar *Energy Materials & Solar Cells*, 2011, 95, 2621.
[38] Y.J. Cho, J. Yong, J.Y. Lee, B.D. Chin, S. R. Forrest, *Organic Electronics*, 2013, *14*, 1081.